$K_{\mu 3}{}^0$ Decay Spectrum*†

D. W. CARPENTER, A. ABASHIAN, R. J. ABRAMS, G. P. FISHER,‡ B. M. K. NEFKENS, AND J. H. SMITH
Department of Physics, University of Illinois, Urbana, Illinois
(Received 11 October 1965)

An experiment has been performed to observe the energy spectrum of the $K_{\mu 3}{}^0$ decay ($K_2{}^0 \to \pi + \mu + \nu$). The observed spectrum indicates that the decay interaction is vector, rather than scalar or tensor, in agreement with the $V-A$ theory of weak interactions. This conclusion is obtained even when energy-dependent form factors are considered. The two form factors (f_+ and f_-) of the vector interaction are found to be consistent with several possible theoretical models for their behavior. If we assume constant form factors, their ratio is found to be $\xi \equiv f_-/f_+ = 1.2 \pm 0.8$. If we assume a $J=1$ intermediate K-π state to predominate in the decay, we find its mass to be $540_{-70}{}^{+140}$ MeV; if $J=0$, we find a mass of $570_{-70}{}^{+160}$ MeV. The data consist of 1371 events obtained from a neutral-beam spark-chamber detection system in which the charged decay products are observed in a magnetic field. The μ is identified by its ability to pass through several interaction lengths of material into a set of range chambers. A branching ratio of $\lesssim 10^{-4}$ is obtained for neutral-current $K_2{}^0$ decays.

I. INTRODUCTION

PRESENT theories of weak interactions are based upon a universal vector minus axial vector ($V-A$) coupling of lepton and baryon currents.[1–4] These theories have been strikingly successful in describing the characteristics of β decay, π decay, μ decay, and μ capture.[5] However, in each of these interactions strangeness is conserved. It is desirable to test experimentally whether the same theories also describe strangeness-changing interactions. The decays of the K mesons provide an excellent opportunity to study the strangeness-changing weak interactions.[6–9]

There are four common decay modes of the $K_2{}^0$ meson[10]:

$$K_2{}^0 \to \pi^\pm + \mu^\mp + \nu, \quad (K_{\mu 3},\ 27\pm 4\%) \tag{1}$$

$$K_2{}^0 \to \pi^\pm + e^\mp + \nu, \quad (K_{e3},\ 34\pm 3\%) \tag{2}$$

$$K_2{}^0 \to \pi^\pm + \pi^\mp + \pi^0, \quad (\tau(+-0),\ 13\pm 2\%) \tag{3}$$

$$K_2{}^0 \to \pi^0 + \pi^0 + \pi^0, \quad (\tau(000),\ 27\pm 4\%). \tag{4}$$

The present experiment is a measurement of the decay spectrum of (1), the $K_{\mu 3}$ decay mode, to study the following problems:

1. The form of the decay interaction; i.e., whether the weak decay is predominantly scalar, vector, or tensor.

2. The behavior of the form factors involved in the strong-interaction part of the decay.

The Feynman diagram for the $K_{\mu 3}$ decay in a theory with local bilinear coupling for the leptons is shown in Fig. 1. The corresponding $V-A$ matrix element may be written[7,11]:

$$M = \tfrac{1}{2}[f_+(q^2)(P_K + P_\pi)_\lambda + f_-(q^2)(P_K - P_\pi)_\lambda] \times [\bar{u}\gamma_\lambda(1+\gamma_5)v], \tag{5}$$

where

$$q^2 = (P_K - P_\pi)^2 = M_K{}^2 - 2M_K E_\pi + M_\pi{}^2, \tag{6}$$

P_K and P_π are the four-momenta of the K and π, M_K and M_π are their masses, and E_π is the energy of the π in the K rest frame. q^2 is the K-π momentum transfer. The terms u and v are the wave functions of the μ and ν. The terms f_+ and f_- are called "form factors" and are functions of q^2 (or equivalently, of E_π) only. Their magnitudes and variations with q^2 are not predicted by weak-interaction theory without recourse to particular models; they depend on the role played by strong interactions in the decay. The assumption of time-reversal invariance implies that f_+ and f_- are relatively real. Because the K and π are both spin-zero particles and have the same intrinsic parity, only vector (not axial-vector) currents will be effective.

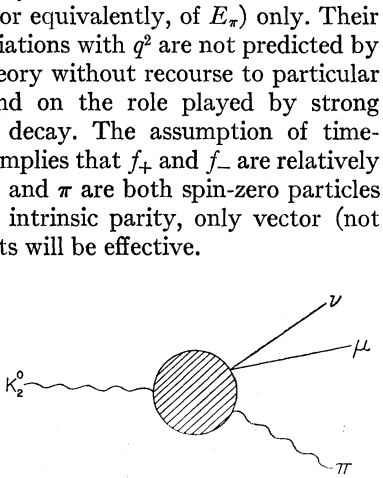

FIG. 1. Diagram for $K_{\mu 3}$ decay.

* This work was supported in part by the U. S. Atomic Energy Commission and the Office of Naval Research.

† Based upon a thesis submitted by D. W. Carpenter in partial fulfillment of the requirements for the doctoral degree at the University of Illinois.

‡ Present address: University of Colorado, Boulder, Colorado.

[1] R. P. Feynman and M. Gell-Mann, Phys. Rev. **109**, 193 (1958).

[2] Brookhaven National Laboratory Report No. BNL 837 (C-39), 1963 (unpublished).

[3] J. D. Jackson, in *Lectures in Theoretical Physics*, edited by W. E. Brittin *et al.* (John Wiley & Sons, Inc., New York, 1962), Vol. 1, p. 263.

[4] L. B. Okun, in *Proceedings of the 1962 International Conference on High-Energy Physics at CERN* (CERN, Geneva, 1962), p. 845.

[5] L. Wolfenstein, in *Proceedings of the 1962 International Conference on High-Energy Physics at CERN* (CERN, Geneva, 1962), p. 821.

[6] P. Dennery and H. Primakoff, Phys. Rev. **131**, 1334 (1963).

[7] J. D. Jackson and R. L. Schult, Tech. Rept. No. 43, Physics Department, University of Illinois, 1962 (unpublished).

[8] J. D. Jackson, Physics Department, University of Illinois, 1961 (unpublished).

[9] William J. Willis, Brookhaven National Laboratory Report No. BNL 837, (C-39), p. 18, 1963 (unpublished).

[10] A. H. Rosenfeld, A. Barbaro-Galtieri, W. H. Barkas, P. L. Bastein, J. Kirz, and M. Roos, Rev. Mod. Phys. **36**, 977 (1964).

[11] S. W. MacDowell, Nuovo Cimento **6**, 1445 (1957).

The differential decay probability in the K rest frame may be found from (5):

$$dw \propto \{[2M_K E_\mu E_\nu - M_K^2(W-E_\pi)]f_+^2 - 2M_\mu^2 E_\nu f_+ f_2 + M_\mu^2(W-E_\pi)f_2^2\} dE_\mu dE_\nu, \quad (7)$$

where

$$f_2 = \tfrac{1}{2}(f_+ - f_-),$$
$$W = (M_K^2 + M_\pi^2 - M_\mu^2)/2M_K = \max E_\pi.$$

Since we do not observe the spins in this experiment, we have summed over the spin directions of the μ and ν in (7). (For experiments in which the μ spin can be observed, one can obtain expressions for the spin direction.[12]) Two independent variables are required to specify the decay configuration (exclusive of orientation) in the K rest frame. We have chosen these two to be E_μ and E_ν. Thus (7) predicts the relative number of decays one would expect to observe with a given E_μ and E_ν. These numbers are referred to as the energy spectrum of the decay.

The K_{e3} decay mode, reaction (2), is also described by (7) if the subscripts (μ) are replaced by (e). In this case, however, the two terms containing M_e become negligible. Since these are the terms involving f_-, only f_+ has an observable effect in K_{e3} decay. By comparing K_{e3} decays with $K_{\mu 3}$ decays, one can thus test whether the variation of f_+ and the magnitude of the coupling constant are the same for decays involving e's as for those involving μ's. Such a difference in the interaction of e's and μ's would be particularly interesting since no differences have been found other than in mass and in coupling to distinct neutrinos. On the other hand, if one assumes identical behavior (μ-e universality), the ratio of $K_{\mu 3}$ to K_{e3} decays can be written in terms of f_+ and f_-.

Thus one may investigate f_+ and f_-, as well as check the universal weak-interaction theory, by three different observations: (1) the $K_{\mu 3}$ and K_{e3} energy spectra; (2) the lepton spin directions in $K_{\mu 3}$ and K_{e3} decay; (3) the branching ratio of $K_{\mu 3}$ to K_{e3}.

Recent experiments[13–16] on K_2^0 decay have shown that the K_{e3} decay spectrum is consistent with the $V-A$ theory, and have given the $K_{\mu 3}$ to K_{e3} branching ratio. No measurement of the spin directions has yet been reported. In the present experiment, we find that the $K_{\mu 3}$ decay spectrum also shows reasonable agreement with the $V-A$ theory with plausible choices of the form factors.

Two decay modes of the K^+ meson are closely related to K_{e3}^0 and $K_{\mu 3}^0$:

$$K^+ \to \pi^0 + \mu^+ + \nu, \quad (K_{\mu 3}^+)$$
$$K^+ \to \pi^0 + e^+ + \nu, \quad (K_{e3}^+).$$

Equation (7) is expected to describe these decays also, except that the form factors may now be different from those of K_2^0 decay. Both $\Delta I = \frac{1}{2}$ and $\Delta I = \frac{3}{2}$ isotopic spin change of the strongly interacting particles may contribute to the decays. There is evidence that the $\Delta I = \frac{1}{2}$ part is dominant ($\Delta I = \frac{1}{2}$ rule).[17] In this case, the form factors would be the same for K^+ as for K_2^0 decay. Thus a comparison of K^+ with K_2^0 decays can test the $\Delta I = \frac{1}{2}$ rule.

The K^+ decays have been measured by several groups.[18–25] These include measurements of both $K_{\mu 3}^+$ and K_{e3}^+ spectra, their branching ratios, and μ-polarization measurements. The polarization of the μ was measured by stopping the μ and observing its decay. Also, the $K_{\mu 3}^-$ spectrum has been observed.[26] In general, the $V-A$ theory with μ-e universality seems adequate for these observations. However, poor statistics and difficulties in the direct observation of the π^0 have not allowed very critical tests to be made.

The decays $K_2^0 \to \mu^+ + \mu^-$ or $K_2^0 \to e^+ + e^-$, while allowed by the common conservation laws, have never been observed.[15,27] This fact is usually incorporated into the $V-A$ theory by postulating the exclusion of neutral currents, i.e., currents which involve only two charged or two neutral leptons. This absence is observed in all other leptonic weak interactions as well. One of the results of this experiment is to set new experimental upper limits of such neutral currents in K_2^0 decays.

The $K_2^0 \to \pi^+ + \pi^-$ decay mode, which apparently violates CP invariance, has now been reported by

[12] N. Cabibbo and A. Maksymowicz, Phys. Letters **9**, 352 (1964).
[13] D. Luers, I. S. Mittra, W. J. Willis, and S. S. Yamamoto, Phys. Rev. **133**, B1276 (1964).
[14] R. K. Adair and L. B. Leipuner, Phys. Letters **12**, 67 (1964).
[15] X. De Bouard, D. Dekkers, B. Jordan, R. Mermod, T. R. Willitts, K. Winter, P. Scharff, L. Valentin, M. Vivargent, and M. Bott-Bodenhausen, Phys. Letters **15**, 58 (1965).
[16] George P. Fisher, thesis, University of Illinois, 1964 (unpublished).
[17] Jack Steinberger, Nevis 125, Department of Physics, Columbia University, 1964 (unpublished).
[18] Gary L. Jensen, C. Thornton Murphy, and Byron P. Roe, Phys. Rev. **138**, B1507 (1965).
[19] G. L. Jensen, F. S. Skaklee, B. P. Roe, and D. Sinclair, Phys. Rev. **136**, B1431 (1964).
[20] F. S. Shaklee, G. L. Jensen, B. P. Roe, and D. Sinclair, Phys. Rev. **136**, B1423 (1964).
[21] John L. Brown, John A. Kadyk, George H. Trilling, Remy T. Van de Walle, Byron P. Roe, and Daniel Sinclair, Phys. Rev. Letters **8**, 450 (1962).
[22] G. Borreani, G. Rinaudo, and A. E. Werbrouck, Phys. Letters **12**, 123 (1964).
[23] D. Cutts, T. Elioff, and R. Stiening, Phys. Rev. **138**, B969 (1965).
[24] U. Camerini, R. L. Hantman, R. H. March, D. Murphree, G. Gidal, G. E. Kalmus, W. M. Powell, R. T. Pu, C. L. Sandler, S. Natali, and M. Villani, Phys. Rev. Letters **14**, 989 (1965).
[25] George Gidal, Wilson M. Powell, Robert March, and Sergio Natali, Phys. Rev. Letters **13**, 95 (1964).
[26] T. H. Groves, P. R. Klein, and V. VanderBurg, Phys. Rev. **135**, B1269 (1964).
[27] M. Kh. Anikina, D. V. Neagu, E. O. Okonov, N. I. Petrov, A. M. Rozanova, and V. A. Rusakov, Zh. Eksperim. i Teor. Fiz. **42**, 130 (1962) [English transl.: Soviet Phys.—JETP **15**, 93 (1962).

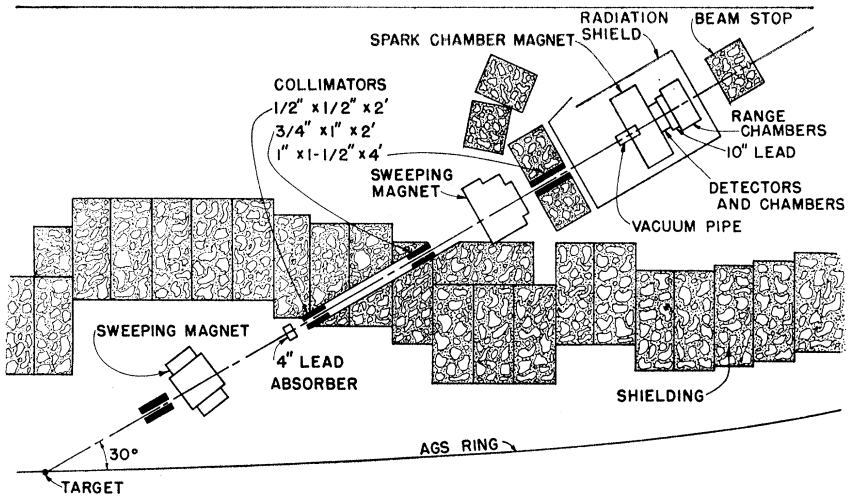

FIG. 2. $K_2{}^0$ beam layout. The neutral beam from the AGS target is defined by the $\frac{1}{2}$ in. wide by $\frac{1}{2}$ in. high and the $\frac{3}{4}$- × 1-in. brass collimators in the shielding wall. The beam clears the final 1- × $1\frac{1}{2}$-in. collimator. The useful $K_2{}^0$ decays occur in the vacuum pipe.

several groups.[15,28,29] The possible observation of a small number of such decays has already been reported by us.[30] These observations, together with the *CPT* theorem (invariance under *CP* plus time reversal), may be evidence for the failure of time-reversal invariance. If this is the case, one has to consider the possibility of relatively complex form factors (f_+ and f_-), and the possibility that the interaction for the decay into $\pi^+\mu^-\nu$ may be different from that for $\pi^-\mu^+\nu$.

II. THE APPARATUS

A beam of neutral particles was set up at the Brookhaven National Laboratory's alternating gradient synchrotron (AGS) as shown in Fig. 2. The first two magnets along the beam deflected charged particles out of the beam. The four inches of lead before the second collimator eliminated most gamma rays. At the detection system, which was 67 feet from the synchrotron target, the beam was composed principally of neutrons, neutrinos, and $K_2{}^0$ mesons, the only known neutrals having lifetimes long enough to let them reach the system. The beam was about $\frac{3}{4}$ in. wide by 1 in. high at this point. The synchrotron operated at a primary energy of 30 BeV for most of the run. For short parts of the run it operated at 20 and 25 BeV. The beam duration was about 0.2 sec at intervals of 3.2 sec. About 600 $K_2{}^0$'s and 20 000 neutrons would pass through the system in a typical beam pulse of 4.0×10^{11} circulating protons.[31] This corresponds to a beam intensity of about 100 $K_2{}^0/(10^{11}$ circ. protons) (μ-sr.).

The detection system is shown in Fig. 3. The useful $K_2{}^0$ decays occurred in a vacuum pipe through which the beam passed. The pipe consisted of an oval $2\frac{3}{4}$-in.-wide by $3\frac{5}{8}$-in.-high stainless steel tube with $\frac{1}{16}$-in. walls. Windows cut in the sides and ends of the pipe were covered with 3-mil Mylar. The vacuum prevented confusion of neutron and K interactions with actual K-decay events. Approximately 10 $K_2{}^0$ decays occurred in the pipe/pulse.

The vacuum pipe was surrounded by a set of spark chambers. The pipe and chambers were placed in a magnetic field of 10.2 kG to allow the measurement of the momenta of the charged decay products. Eleven chambers, each with an 8×6-in. high active area, where located to each side of the pipe. Ten chambers, 23 in. wide × 7 in. high, were located beyond the pipe. Each of these 32 chambers were two gap chambers with three plates of 1-mil aluminum foil, and two sheets of 1-mil Mylar to contain neon gas. The foil and Mylar were glued to Plexiglas frames.

Beyond the magnet was a system of chambers and absorbers in which the identification of the decay products was made. Of the charged decay products of the $K_2{}^0$ only the μ can frequently pass through large amounts of material. Thus, we may preferentially select $K_{\mu 3}$ decays by requiring one of the charged particles to pass through the 10 in. of lead after it leaves the magnet.

The μ was observed in a set of 24 range chambers beyond the lead. Each of these chambers was a two-gap spark chamber made of three $\frac{1}{8}$ × 48-in.-wide by 36-in.-high aluminum plates glued to Plexiglas frames. In front of each of the first 20 chambers was a $\frac{3}{8}$-in. brass plate; the last 4 chambers had two plates in front of each. Usually, the μ stopped somewhere in the plates and the range of the track could be measured. In order to enter these range chambers, a μ would require a momentum of over 540 MeV/c. A π of the same momentum would have to pass through 1.8 interaction

[28] J. H. Christenson, J. W. Cronin, V. L. Fitch, and R. Turlay, Phys. Rev. Letters **13**, 138 (1964).
[29] W. Galbraith, G. Manning, A. E. Taylor, B. D. Jones, J. Malos, A. Astbury, N. H. Lipman, and T. G. Walker, Phys. Rev. Letters **14**, 383 (1965).
[30] A. Abashian, R. J. Abrams, D. W. Carpenter, G. P. Fisher, B. M. K. Nefkens, and J. H. Smith, Phys. Rev. Letters **13**, 243 (1964).
[31] H.-J. Gerber, G. Fisher, R. Jones, and A. Wattenberg, Tech. Rept. No. 39, Physics Department, University of Illinois, 1962 (unpublished).

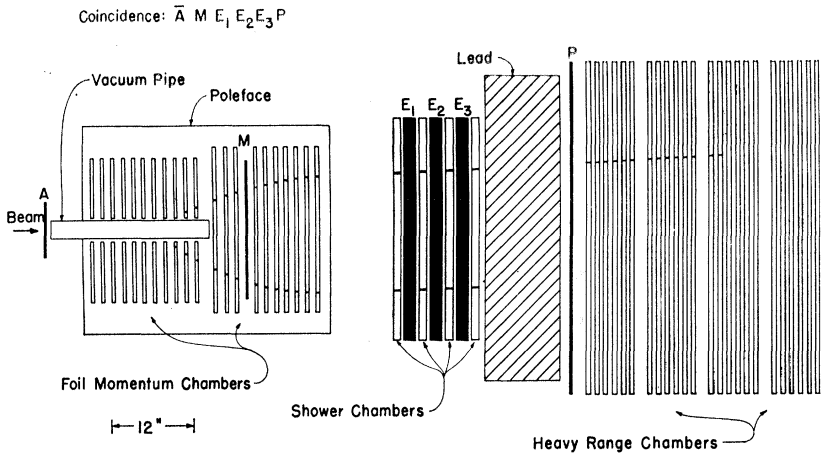

FIG. 3. Top view of the K_2^0 detection system. The scintillation counter A is about 67 ft. from the AGS target, and 56 in. from the last collimator.

lengths of material before entering the first range chamber. Thus, a π is likely to interact and not reach the range chambers. This material consisted of 320 g/cm^2 of lead, 25 g/cm^2 of brass, 7 g/cm^2 of aluminum, and 6 g/cm^2 of plastic. The interaction length value (1.8) is based on tables compiled by Williams.[32] If the π did not interact, its range would be indistinguishable from the μ. Electrons do not get through the lead.

The chambers were triggered when a coincidence between counters M, $E1$, $E2$, $E3$, and P was observed, with A in anticoincidence (see Fig. 3). M is a $\frac{1}{8} \times$ 20-in. plastic scintillation counter in the magnet, beyond the pipe. $E1$, $E2$, and $E3$ are three 12 $\times$ 32-in. detectors between the magnet and the lead. P is any one of a $\frac{3}{8} \times$ 48-in.-wide by 24-in.-high array of six scintillators between the lead and the range chambers. The anticoincidence counter A is a $\frac{1}{8} \times 8 \times 8$-in. scintillator placed in the beam just in front of the vacuum pipe. Thus triggered events should have at least one visible track coming from the vacuum pipe region and at least one track, which was likely to be a μ, entering the range chambers.

The detectors $E1$, $E2$, and $E3$ were three identical detectors designed as shower detectors to be used to identify electrons from the K_{e3} decay. These were used in that way in the experiment described by Fisher.[16] They consisted of five layers of $\frac{1}{8}$-in. scintillator with $\frac{3}{32}$-in. lead sheets between each layer. The beam passes through a $1\frac{1}{2}$- $\times$ $2\frac{1}{2}$-in. hole in these detectors. In this experiment, the trigger level of these detectors was set to accept a single minimum ionizing particle so a shower was not required. Four 4-gap spark chambers designed to observe electron showers were in operation between these detectors during part of this experiment. They were used in this experiment only for studies of contamination by K_{e3} events.

One camera was used to photograph both the top and side view of the foil chambers in the magnet through a system of mirrors. A second camera took a 10° stereo pair photograph of the top of the range and shower chambers.

A trigger from the coincidence system was received on an average of 1.0 times per synchrotron pulse. Only the first trigger in any beam pulse was used to fire the chambers. About two-thirds of these triggers were due to K decays. Most of the rest were caused by neutron interactions in the scintillator (M) in the magnet. In about half of the K decays one of the two charged tracks did not go through four or more chambers in the magnet.

More detailed descriptions of the apparatus are given elsewhere.[16,33]

III. SCANNING AND MEASURING OF THE FILM

The photographs of the momentum chambers in the magnet were scanned to find measurable decays (V's) from the vacuum. A picture was accepted for measurement if each of the two tracks of the V had sparks in 4 or more chambers and if the tracks had opposite curvatures. Also, we required that each accepted event had a track with sparks in at least two chambers of the corresponding range chamber photograph. Two scans of the 40 000 pictures yielded 6965 (18%) events which satisfied the above criteria.

The remainder of the pictures consisted of several types. The largest fractions were interactions of beam particles with the scintillator (M) in the magnet (35%) and pictures in which only one track was measurable (30%). There were also pictures with V's, but without the required track in the range chamber (6%); pictures with no measurable track (5%); pictures with V's from the beam, but obviously from before or after the vacuum pipe (4%); pictures with more than two tracks (1%); and pictures with V's well outside the beam (less than 1%).

[32] Robert W. Williams, Rev. Mod. Phys. **36**, 815 (1964).

[33] D. W. Carpenter, thesis, Department of Physics, University of Illinois, 1965 (unpublished).

The sparks in the selected events were digitized on punched cards with a Hydel measuring machine, and analyzed on an IBM 7094 computer.[34] Each pair of tracks was fitted to two helices. The distance of closest approach of the two was found and this point of closest approach was taken to be the decay point.

Of the 6965 measurements, 392 ($5\frac{1}{2}\%$) failed to have a closest approach distance within a 0.3-in. limit. These failures were largely due to scattering in the vacuum pipe walls and in the frames of the small foil chambers, though most tracks missed this material. Another 186 ($2\frac{1}{2}\%$) failed to fit helices well enough (0.025-in. rms deviation perpendicular to the field, 0.035 in. along it), even after repeated measurements.

The position of the decay was also required to meet certain criteria. We found 132 events (2%) decayed outside the beam. A large number of events, 1326 (19%), were too close to, or just beyond the end of the pipe. Another 1047 (15%) were near the front of the magnet and not used because of the difficulty of analysis of tracks in a rapidly changing magnetic field. These limits reduce the useful length of the vacuum pipe to 17.3 in.

We are left with 3882 events (56% of those measured) with decays in the acceptable region. The background of events other than K_2^0 decays in this sample seems to be negligible. Interactions of beam particles in the anticoincidence counter cause a negligible background.

The laboratory momenta of the tracks (typically about 1 BeV/c) were measured to about 3% accuracy. When the decays are transformed to the center-of-mass system, the particle energies are determined with an rms error of 5 MeV.

The measurements in the magnet of the two as yet unidentified tracks must be correlated with tracks observed in the range chambers. For this purpose, the expected positions and ranges in the range chambers were computed[35] for each of the two measured tracks on the assumption that each of the two were μ's. The tracks in the range chamber were then compared with the expected values to see which track, if either, was consistent with the assumption that it was a μ. Tracks which pass through all 24 chambers (over 4 interaction lengths for a π) were also accepted as μ's.

Of the 3882 acceptable decays in the magnet, 1758 were thus identified as $K_{\mu 3}$ decays. Nineteen events in which both tracks met the μ identification requirements were discarded. The remainder were mostly tracks which fell more than 80 MeV/c short of the predicted range or went out the sides of the chambers.

Pions which happen to go their full range without a nuclear collision or which decay in flight will, in general, be mistakenly labeled μ's. About 8% of the π's are labeled μ's because of these effects. Since the decays of the K_2^0 involve three times as many charged π's as μ's, about 19% of the identified events are incorrectly identified. This contamination is the major background problem in this experiment. Part of the contamination is removed by techniques described in the next section.

IV. KINEMATICS, AMBIGUITIES, AND EFFICIENCIES

There are 1758 candidates for $K_{\mu 3}$ decays. For each candidate the momentum in the laboratory has been measured for both tracks, and one of the tracks has been tentatively identified as a μ as described in III. With this information we can proceed to calculate the energies of the decay particles in the rest frame of the K (the center-of-mass system) in order to analyze the results.

The momentum of the ν in the center-of-mass system can be calculated uniquely:

$$P_\nu^* = (M_K^2 - M_c^2)/2M_K, \tag{8}$$

where

$$M_c^2 = E_c^2 - P_c^2 = (E_\pi + E_\mu)^2 - (\mathbf{P}_\pi + \mathbf{P}_\mu)^2,$$

the effective mass squared of the two charged particles. The asterisk denotes center-of-mass quantities.

The direction (but not the momentum) of the K is known. This direction, the direction of the beam, was found within 0.1° by fitting the set of measured decay points to a straight line. We may calculate the component of the ν momentum which is transverse (T) to the beam:

$$\mathbf{P}_{\nu T}^* = \mathbf{P}_{\nu T} = -\mathbf{P}_{cT} = -(\mathbf{P}_\pi + \mathbf{P}_\mu)_T. \tag{9}$$

The longitudinal (L) component is then:

$$P_{\nu L}^* = \pm (P_\nu^{*2} - P_{\nu T}^{*2})^{1/2}. \tag{10}$$

The twofold sign results in an ambiguity in the laboratory energy of the K and also in the center-of-mass energies of the π and μ. One finds:

$$\gamma \equiv E_K/M_K = \frac{[(M_K - P_\nu^*)E_c \pm P_{\nu L}^* P_{cL}]}{(E_c^2 - P_{cL}^2)}. \tag{11}$$

There are, consequently, two values of γ with which to transform the π and μ energies into the center-of-mass system.

Events for which $P_\nu^* < 0$, or for which $P_{\nu T}^* > P_\nu^*$ (beyond reasonable measurement errors) are not consistent with a $K_{\mu 3}$ decay. Of the identified events, 59 ($3\frac{1}{2}\%$) had such inconsistencies by more than 30 MeV/c. These events were discarded.

The events which are kinematically inconsistent with $K_{\mu 3}$ decay are an indication of the amount of contamination resulting from the mistaken identification of a π as a μ. Most of these events are K_{e3}'s; the inconsistency is an effect of an energy release which is larger than that present in $K_{\mu 3}$ decays. From the K_{e3} events of Fisher,[16]

[34] Computer operated by the Department of Computer Science, University of Illinois, partially supported by a grant from the National Science Foundation. Film measuring equipment prepared by R. D. Sard.

[35] R. M. Sternheimer, Phys. Rev. **117**, 485 (1960).

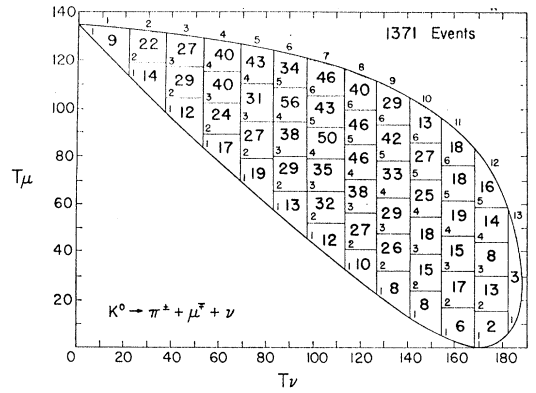

FIG. 4. The lower E_K solutions are grouped into 55 equal sized bins on the phase-space diagram. The small numbers above the strip are the strip numbers; those in the corners of the bins are bin numbers. The large numbers are the numbers of events falling in each bin. The kinetic energy units are MeV.

we estimate that one-third of the K_{e3} contamination events will be inconsistent with $K_{\mu 3}$ decay. Thus, the two-thirds of the K_{e3} contamination not eliminated by the inconsistency are still in the data. This implies a 7% ($2\times 3\frac{1}{2}$%) contamination. Another check on the amount of K_{e3} contamination is available by observing the behavior in the shower chambers of the track that is supposed to be a π from a $K_{\mu 3}$ decay. If it appears to shower, it was probably an electron; and the event was a K_{e3} decay. In the short part of the run in which the shower chambers were in operation, we observed such a shower in about 3% of the events in which the track in question entered the shower chambers. Another estimate is available from the assumption that 8% of the π's will be called μ's (see II). This implies 8% times the $K_{e3}/K_{\mu 3}$ branching ratio, or 10%. We believe that the K_{e3} contamination in the data is (7 ± 4)%.

The events in which the π from a $K_{\mu 3}$ was mistaken for a μ are also a contamination. These events are not likely to be kinematically inconsistent. An estimate of a 8% contamination follows directly from the assumption that 8% of the π's will be labeled μ's. A crude check is provided by the number (19) of events in which there are apparently two μ's. This implies about 3% contamination. We believe that the incorrectly identified $K_{\mu 3}$ contamination is (6 ± 3)%.

The possibility of a similar contamination by $\tau(\pi^+\pi^-\pi^0)$ decays is eliminated by excluding all events which are kinematically consistent with τ decay.[36] This process eliminated 328 events. Of these, only about one-third are actually τ decays; the rest would have been good $K_{\mu 3}$'s. The efficiency calculation takes into account this loss of good events. The τ contamination would have been particularly serious because all such events would group together at the high E_ν region of the spectrum when interpreted as $K_{\mu 3}$'s.

There remain 1371 events for the final analysis.

Each event has two possible center-of-mass solutions for the decay particle energies. We arbitrarily chose the solution which corresponds to the lower laboratory energy of the decaying K, or lower γ in (11). We shall see that this choice results in picking the correct solution about four times as often as the wrong one.

These "lower E_K" solutions for the energies of the ν and μ for the 1371 events have been placed in bins on a phase-space diagram (Fig. 4). The diagram has been divided into 55 equal size bins, each about 15 MeV wide. The bins are arranged so that the two ambiguous solutions for any event would lie in the same vertical strip (they have the same T_ν).

In order to compare the data with the theoretical predictions for the densities expected in each bin, three corrections must be made:

(1) a correction for the detection efficiency at each point in the plot,

(2) a correction for the error introduced by arbitrarily taking the lower E_K solutions,

(3) a correction for the deletion of events which are kinematically possible τ decays.

The efficiency was calculated for each bin by a Monte Carlo event-generating program. Ten thousand events were generated in each bin by picking random points in the bin, giving each event a random orientation in the center of mass, and a random position along the vacuum pipe. The K energy was picked at random from a distribution weighted according to the beam-energy spectrum of decaying K's. This K-beam energy spectrum was obtained from the data in a manner explained in the Appendix.

For each generated event, the μ was tested to see whether it would trigger the system and be identifiable. This meant that the μ must go through the scintillators E and P, reach at least chamber 2 of the range chambers, and either stop in the chambers, go out the sides after coming within 4 chambers of its full range, or go through all 24 chambers. For each μ which passed the test, the accompanying π was tested to see if it would be measurable; i.e., if the π would pass through 4 or more foil chambers. The number of trials passing both tests was recorded.

The resulting laboratory momenta for each successful trial were tested to see if the trial could have been interpreted as a τ decay (the same test given the real events). If it could, the trial was not counted.

For each of the remaining successful trials, the center-of-mass solution corresponding to the second (wrong) of the two ambiguous solutions was calculated. If the second solution had a lower E_K than the actual E_K being tested, a record was kept of the bin in which the second solution would appear (always a bin in the same strip). This corresponds to the lower E_K method of selecting

[36] The criterion for elimination of possible τ decays is $(P_0')^2 > -7000$. $(P_0')^2$ is a quantity greater than zero for actual τ decays. The use of -7000 rather than 0 allows for measurement error (about 30 MeV/c for the π^0). The quantity $(P_0')^2$ is defined by Luers *et al.* (Ref. 13). It is closely related to $(P_{\nu L}^*)^2$ defined in Eq. (10).

a solution from the data events. Alternatively, if the E_K being tested was lower, the record was kept that the correct bin would be chosen.

The efficiency can now be expressed as a two-dimensional matrix for each strip of bins at one neutrino energy: $E_{jk}{}^i$, where (i) is the strip number, (k) is the bin in that strip in which the actual solution occurs, and (j) is the bin (also in strip, i) in which the solution chosen by picking the lower E_K solution occurs. For example, $E_{12}{}^6$ is the fraction of those K's which decay with c.m. energies appropriate to bin 2 in strip 6 which would trigger the system, would be measured and identified as $K_{\mu 3}$'s and would be placed in bin 1 (strip 6) when the lower E_K solution is plotted.

If the theoretical number of decays occurring in bin (i,k) is $T_k{}^i$, then the number of events observed in bin (i,j) in the experiment should be:

$$D_j{}^i = C \sum_k E_{jk}{}^i T_k{}^i. \tag{12}$$

(Since we do not measure absolute rates, the $T_k{}^i$ have meaning only relative to each other. The constant C is used to normalize the arbitrarily scaled T to the data.) In Sec. V, the data are analyzed by taking various models for $T_k{}^i$ and computing the expected $D_j{}^i$ from (12). The results are then compared with the observed data (Fig. 4).

The efficiency matrices may be inverted. This results in:

$$T_k{}^i = \frac{1}{C} \sum_j (E_{jk}{}^i)^{-1} D_j{}^i.$$

If $D_j{}^i$ is the observed data, then $T_k{}^i$ will be the data with corrections for efficiencies and ambiguities. Figure 5 shows the results obtained in this way. This method is particularly useful in visualizing the form of the matrix element implied by the data.

The relation between D and T for strip 5 is shown as an example:

$$D_j{}^5 = \sum_k E_{jk}{}^5 \qquad T_k{}^5 \qquad C \tag{13}$$

$$\begin{pmatrix} 19 \\ 27 \\ 31 \\ 43 \end{pmatrix} = \begin{pmatrix} 2.72 & 0.04 & 0.00 & 0.00 \\ 1.35 & 4.78 & 0.08 & 0.02 \\ 1.19 & 1.69 & 7.20 & 0.09 \\ 0.91 & 1.40 & 1.60 & 10.45 \end{pmatrix} \begin{pmatrix} 61 \\ 32 \\ 20 \\ 23 \end{pmatrix} \quad (0.114)$$

Here, E is expressed in percent. [The constant C (0.114) has been chosen arbitrarily to be $1/E_{11}{}^1$ which will scale T such that $T_1{}^1 = D_1{}^1$.] The largest numbers in the efficiency matrix are on the diagonal, indicating that most of the solutions are being chosen correctly. The off-diagonal elements represent the wrong choices. A table of all of the E matrices is given in Ref. 33.

The sum of one column of any E is the total detection efficiency for that bin; for example, we see from the numbers above that the total efficiency for bin (5,2) is 7.91%. These efficiencies range from about 10% at high μ kinetic energies to 1% at $T_\mu = 0$. The efficiency is approximately linear in T_μ between these extremes. The chief cause of this effect is that the additional energy available to the μ will give it a better chance to penetrate the lead wall. This chance also gets better as γ_K increases. If $\gamma_K < 1.6$, even the most energetic μ's will not be detected. A rapid decrease in the beam intensity as γ_K increases is the reason that the lower E_K solution is the correct one in about 80% of the events (see Fig. 10).

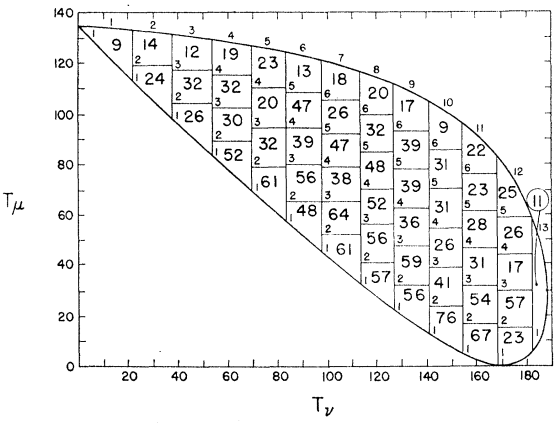

FIG. 5. The raw data of Fig. 4 are corrected for the efficiencies and ambiguities. The normalization has been arbitrarily chosen such that the number in bin (1,1) (the bin with no ambiguity) is the same as it was in the raw data.

A second method of handling the ambiguity was used as a check on the method described above. This method was to accept only those events for which the two solutions for $T_\mu{}^*$ were within 16 MeV of each other. These relatively unambiguous events were always interpreted in nearly the right place in spite of the ambiguity. However, this method allows only about one-half of the data to be used. The efficiencies appropriate to this method of selection of the data were computed at the same time as the efficiencies described above. The results obtained by this method are consistent with the results obtained by the lower E_K method.

V. ANALYSIS OF THE DECAY INTERACTION

In this section, the data are compared with various theoretical models of the decay interaction. First, it is verified that the vector $(V-A)$ model does fit the data better than other proposed models. Then we examine the behavior of the form factors f_+ and f_- which occur in the vector theory.

A. Type of Interaction

The vector model is one of three forms allowed by Lorentz invariance with the assumption of a local, bilinear coupling of the μ and ν.[3,8,11] The three are scalar, vector, and tensor (S, V, and T). For the vector interaction, the energy spectrum involves two form

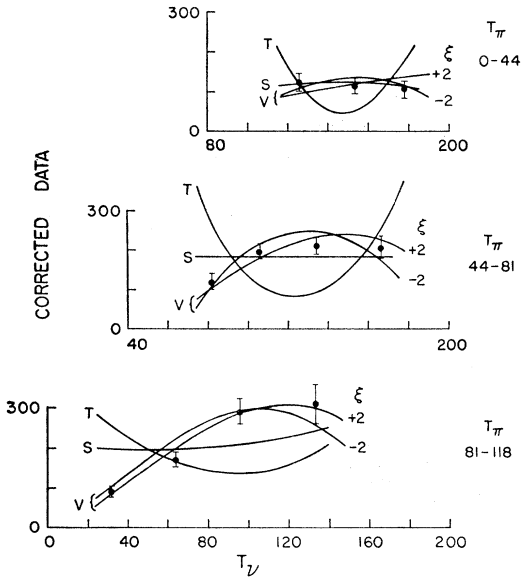

FIG. 6. Comparison of S, V, and T curves with data. Comparison of data with theory along strips of constant T_π can distinguish between S, V, and T interactions without reference to form-factor variations. Theoretical curves for S, T, and two V possibilities are compared with the corrected data in three regions of T_π. The theory is normalized to the data independently in each region.

factors [Eq. (7)]. For the corresponding scalar and tensor interactions, the energy spectra involve only one form factor each[11]:

$$dw_S \propto f_S^2(q^2)(W-E_\pi)dE_\mu dE_\nu, \tag{14}$$

$$dw_T \propto f_T^2(q^2)\{[(E_\mu-E_\nu)^2-M_\mu^2] \times(W-E_\pi)M_k+2M_\mu^2E_\nu^2\}dE_\mu dE_\nu. \tag{15}$$

The form factors again are arbitrary functions of q^2 (or of E_π). We may distinguish between S, V, and T by making the comparison of the data with the theoretical curves along strips of constant E_π. Along such strips, the form factors do not vary because they are functions of E_π only. The data along three such strips are shown in Fig. 6 along with theoretical curves for S, V, and T. The theory has been normalized to the data in each strip independently. We see that only V gives reasonable agreement regardless of possible form-factor variations.

Quantitative comparisons (χ^2 tests) between S, V, and T interactions, assuming linearly varying form factors, show that the vector form is preferred by $\gg 10^6/1$. [The best scalar fit occurs with $f_S=1-0.129\times(q^2/M_\pi^2)$ where $\chi^2/\mathrm{DF}=3.27$ with the number of degrees of freedom DF = 53.]

Thus the decay interaction is established as being predominantly vector. This is consistent with all other known weak interactions. Mixtures of S, V, and T are theoretically possible, but have not been necessary in other interactions even where very critical tests could be made.

In what follows, we assume that the interaction is pure vector, and turn our attention to the form factors. All quantitative tests below are made by comparing the theoretical predictions (with efficiency and ambiguity corrections as described in IV) to the raw data (Fig. 4), rather than using values of the corrected data from Fig. 5 as above.

B. Constant Form Factors

The first investigation of the form factors is made assuming them to be constant. In this case, only one parameter,

$$\xi \equiv f_-/f_+, \tag{16}$$

is present. Maximum likelihood and χ^2 tests were made by comparing (using Poisson statistics) the number of events in each bin with the number expected as a function of ξ. The results are shown in Fig. 7. The maximum likelihood occurs at $\xi=1.3\pm0.4$ with $\chi^2/\mathrm{DF}=0.99$ and DF (degrees of freedom) = 53. These results are based on counting statistics only; corrections must still be made for other uncertainties including possible systematic errors. The χ^2 percentile is 50% (probability that one should get a better fit); i.e., a reasonable fit.

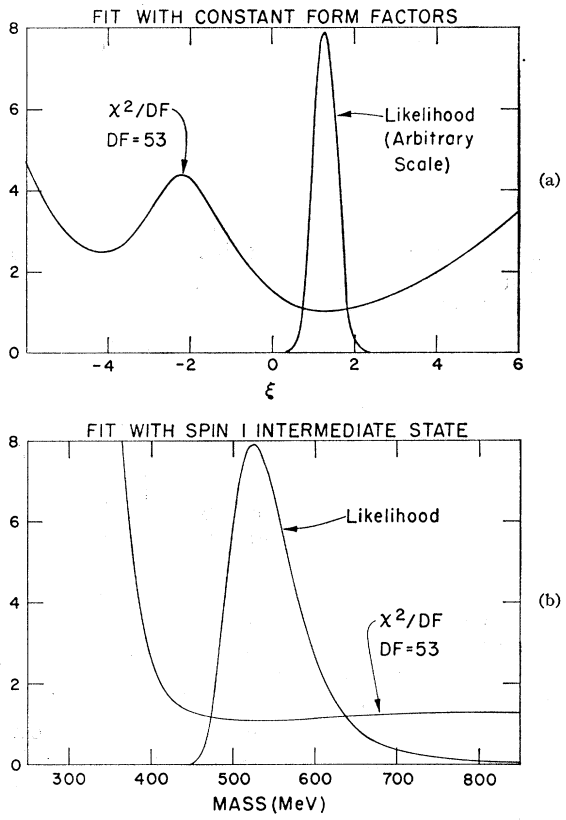

FIG. 7 (a) χ^2/DF and likelihood curves for the one-parameter ($\xi\equiv f_-/f_+$) fit assuming constant form factors in the vector theory. (b) Similar curves for the one-parameter (M) fit assuming a $J=1$ intermediate state of mass M.

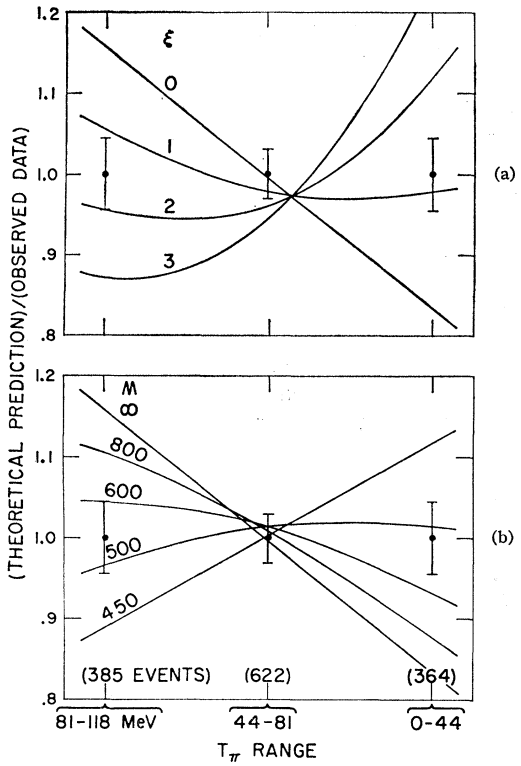

FIG. 8. The (theoretical prediction)/(observed data) is shown in three T_π energy ranges by the solid lines. The data are shown by the points. In (a), the parameter is $\xi \equiv f_-/f_+$. In (b), the parameter is M, the mass of an intermediate spin-1 state.

(The use of only the relatively unambiguous data, as described at the end of Sec. IV, gives $\xi = 1.6 \pm 0.5$.)

There are several sources of possible systematic error. The contamination by misidentified events is estimated to contribute an error in ξ of 0.1 ± 0.4. (A uniformly distributed background subtraction of 16% of the raw data would change the best fit ξ by -0.1.) Uncertainties in matching the calculated efficiencies to the actual triggering and scanning efficiencies, uncertainties in the magnetic field measurements, and uncertainties in the K-beam spectrum contribute errors of about ± 0.2 each.

Thus for constant f_+ and f_-, we find

$$\xi = 1.2 \pm 0.8. \tag{17}$$

The $K_{e3}{}^0$ data cannot be used to compare with this value of ξ because only f_+ is effective there. However, the branching ratio $R(K_{\mu 3}/K_{e3})$ can be computed assuming constant f's and μ-e universality:

$$R = 0.65 + 0.124\xi + 0.019\xi^2. \tag{18}$$

This ratio has been measured by Luers *et al.*,[13] who obtain $R = 0.73 \pm 0.15$, and by Adair and Leipuner,[14] who obtain 0.81 ± 0.19. We combine these to get $R = 0.77 \pm 0.12$. With (18), this implies $\xi = 0.8 \pm 0.8$ (or -7.4 ± 0.8).

The predominant features of the data which are useful in obtaining ξ are shown in Fig. 8(a). The data are divided into three regions of π energy. For each region, the theoretical prediction divided by the observed number of events is shown for various values of ξ along with data points. While the distribution of events within a region also changes with ξ, the changes are not nearly so marked as these between regions (see Fig. 6). The likelihood calculation (Fig. 7) includes both effects.

C. $J=1$ Intermediate State

If one assumes that the strong part of the interaction is dominated by a sharp K-π resonance or intermediate state, one can use dispersion theory to calculate the form factors in terms of the mass (M) of the state.[3,6,8,37] For a $J=1$ state, the relations are:

$$f_+(q^2) = f_+(0)/(M^2 - q^2), \tag{19}$$

$$f_-(q^2) = -f_+(q^2)[(M_K{}^2 - M_\pi{}^2)/M^2]. \tag{20}$$

The data were fitted with M as a free parameter. The results are shown in Fig. 7(b). The best fit occurs at $M = 530_{-40}{}^{+50}$ MeV, with $\chi^2/\mathrm{DF} = 1.11$. The χ^2 percentile is 73%, a reasonable fit. (The relatively unambiguous data alone give $M = 540_{-60}{}^{+130}$.)

The contamination is estimated to contribute an error in M of $-(10_{-40}{}^{+50})$ MeV. (A 16% uniform background subtraction raises M by 10 MeV.)

The efficiency, field, and beam spectrum uncertainties each contribute errors of about ± 20 MeV.

Thus we find:

$$M = 540_{-70}{}^{+140} \text{ MeV}. \tag{21}$$

The mass of 540 MeV for the K-π intermediate state is lower than one might expect. If $M < M_K + M_\pi$ (637 MeV), it would be a bound state. If $M < M_K$ (498 MeV), the K would decay into the bound state. The known K-π resonances occur at 891 MeV ($J=1$) and 725 MeV (J unknown),[10] both too high for the observed effect. The discrepancy could mean that a single sharp resonance does not dominate the interaction as assumed in (19) and (20). For example, both the 725 and 891 resonances may be effective. The data can be fit well with this combination or with either mass combined with a very high mass.

The assumption of a spin-1 intermediate state can also be applied to $K_{e3}{}^0$ decay. The results of Luers *et al.*,[13] are presented in their Fig. 6(a). From the figure, it appears that their data are consistent with M from about 500 MeV to infinity with the best agreement near 700 MeV.

The ratio $R(K_{\mu 3}/K_{e3})$ predicted assuming μ-e universality is quite insensitive to M. A calculation shows that R is 0.65 for M from infinity to 460 MeV. R rises

[37] J. L. Acioli and S. W. MacDowell, Nuovo Cimento 24, 606 (1962).

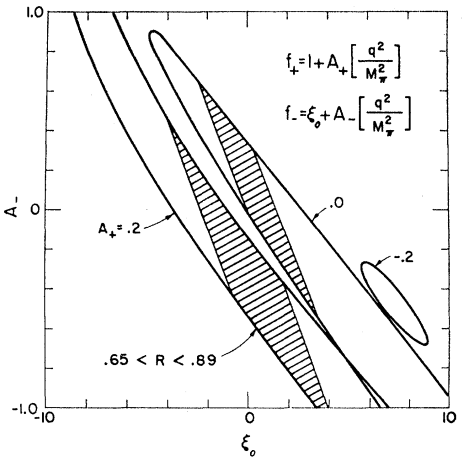

FIG. 9. Three-parameter fit with linearly varying form factors. Regions of reasonable agreement with the data at various values of A_+ are shown. The measured value of $R(K_{\mu 3}/K_{e3})$ would restrict the allowed values of the parameters to the shaded portions of the regions shown. $R=0.65$ is the left side of the regions; 0.89 is the right.

to 0.67 at 400 MeV, and to 0.72 at 360 MeV (at 358 MeV$=M_K$-M_π, the resonance moves into the physical region). The measured value of $R(0.77\pm0.12)$ is consistent with all of these values.

Again the predominant features of the data useful in obtaining M may be shown by dividing the data into three regions of π energy as shown in Fig. 8(b). It is evident from the figure why the errors quoted are skew.

Very little information is gained from the distribution within each region. From (20) we see that the ratio of the form factors is constant even though they are individually varying:

$$f_-(q^2)/f_+(q^2)=-(M_K^2-M_\pi^2)/M^2=\xi_M=\text{const.} \quad (22)$$

But this ratio varies only from 0 at $M=\infty$ to -1.1 at $M=450$ MeV. Thus the behavior within each π-energy region is nearly independent of M (see Fig. 6). The value $M=540$ MeV gives $\xi_M=-0.8$.

D. Linearly Varying Form Factors

If we let both form factors vary linearly with q^2, we may specify the theory in terms of three parameters: ξ_0, A_+, and A_-:

$$f_+(q^2)=1+A_+(q^2/M_{\pi^+}^2), \quad (23)$$

$$f_-(q^2)=\xi_0+A_-(q^2/M_{\pi^+}^2). \quad (24)$$

Here, $\xi_0=f_-(0)/f_+(0)$, while A_+ and A_- give the rate of variation of f_+ and f_-. The range of (q^2/M_π^2) is 0.573 to 6.585, increasing as T_π decreases.

Figure 9 displays the results of the three-parameter fit. For various values of A_+, curves are drawn along lines at which the combination of A_+, A_-, and ξ_0 gives $\chi^2/\text{DF}=1.50$ (DF$=51$). The areas inside the loops give better fits. There are more allowed regions with A_+ above 0.2 which lie below the portion of the graph shown. The best fit occurs at $\xi_0=5.6$, $A_+=-0.01$, and $A_-=-0.6$ with $\chi^2/DF=0.92$ (36%). The permitted deviations are large and strongly correlated, as shown on the graph. The edges of the curves are intended to represent reasonable error limits at the various values of A_+.

The measured value of $R(K_{\mu 3}/K_{e3})$ will restrict the values of the parameters allowed in Fig. 9. The shaded areas are the regions allowed by $R=0.77\pm0.12$ at the values of A_+ indicated. (The calculations are based on expressions given by Jackson and Schult.[7])

It is apparent that three parameters are too many to be very well determined with the present data. Independent measurements such as R, polarizations, or K_{e3} spectra are needed to reduce the number of free parameters.

E. $J=0$ Intermediate State

One can assume a $J=0$ intermediate state similar to the $J=1$ state discussed in Sec. V C above. In this case, the predictions for the form factors are[3,8,37]:

$$f_+(q^2)=f_+(0), \quad (25)$$

$$f_-(q^2)=f_+(0)(M_K^2-M_\pi^2)/(M_0^2-q^2), \quad (26)$$

where M_0 is the mass of the state. The best fit occurs at $M_0=570_{-70}^{+160}$ MeV with $\chi^2/\text{DF}=1.03$ (57%).

F. Conserved Vector Current

The conserved vector current theory[3,8,38] predicts the following relation:

$$f_-(q^2)=-[(M_K^2-M_\pi^2)/q^2]f_+(q^2). \quad (27)$$

One form factor is given in terms of the other, but the other may vary in any way. To test the theory, we have assumed

$$f_+(q^2)=1+A_+(q^2/M_\pi^2). \quad (28)$$

The best fit then occurs with $A_+=0.20$, but it is an extremely poor fit with $\chi^2/\text{DF}=2.32$. Thus the conserved vector current for strangeness-changing decays seems ruled out. This result was expected on the basis of previous data.[3,8]

G. Time-Reversal Invariance

In the above discussions, we have assumed that time-reversal invariance holds. As mentioned in Sec. I, recent experiments have indicated that this assumption may not be true in K^0 decays. We have investigated several possible tests of the invariance in the $K_{\mu 3}$ decay.

(1) A violation of time-reversal (T) invariance would allow f_- and f_+ to be relatively complex. We find that the addition of a complex parameter does not improve the goodness of fit significantly.

[38] M. L. Goldberger and S. B. Treiman, Phys. Rev. **110**, 1478 (1958).

(2) T invariance (combined with the CTP theorem) requires that the rate of $K_2^0 \to \pi^+\mu^-\nu$ be equal to $K_2^0 \to \pi^-\mu^+\nu$. We find $R(\mu^+/\mu^-) = 1.08 \pm 0.06$. However, the detection system is known to have some asymmetries. The run was done with the magnetic field down for the first half; up for the second. The ratio was different for the two halfs: R(field down) $= 0.96 \pm 0.09$, R(field up) $= 1.21 \pm 0.09$. Since these differences are not completely understood,[16] the apparent deviation of R from 1 may not be significant. There is no observable difference in the decay spectra between the field-down and field-up data.

(3) T-invariance violation would permit the form factors to be different for $\pi^+\mu^-\nu$ decay than for $\pi^-\mu^+\nu$ decay. The differences we see are small enough that they have a negligible effect on the form-factor analysis described above. For example, the two sets of data with oppositely charged products give the same spin-1 intermediate state mass to within 2 MeV.

H. Neutral Current Decays

Another apparent phenomenological rule, the prohibition of neutral leptonic currents, is examined. This rule would prohibit the decays $K_2^0 \to \mu^+ + \mu^-$, $e^+ + e^-$, and $\mu^\pm + e^\mp$. Among the events of both the $K_{\mu 3}$ run and the accompanying K_{e3} experiment, we find: 0 candidates for e^+e^-; 1 candidate for $\mu^+\mu^-$; 3 candidates for $\mu^\pm e^\mp$. In each case, the event satisfies the decay kinematics. The reconstructed K mass is between 480 and 520 MeV and the K direction is within 20 mrad of the beam direction. Also, in each case, the given identity of the products cannot be ruled out. In no case, however, can both products be identified by their behavior in the shower or range chambers. Thus the above numbers are upper limits. The branching ratio obtained is

$$B\left(\frac{K_2^0 \to ee,\ \mu\mu,\ \text{or}\ \mu e}{K_2^0 \to \text{charged modes}}\right) \lesssim 10^{-4}. \qquad (29)$$

The corresponding partial lifetime is

$$\Gamma(K_2^0 \text{ neutral current}) \gtrsim 6 \times 10^{-4} \text{ sec}.$$

The decay $K^+ \to \mu^+ + \nu$ (a charged current) has a partial lifetime of

$$\Gamma(K^+ \to \mu^+ + \nu) = 2 \times 10^{-8} \text{ sec}.$$

Since the phase space is comparable with $K^0 \to \mu^+\mu^-$, we conclude

$$\left(\frac{\text{neutral current coupling constant}}{\text{charged current coupling constant}}\right)^2 \lesssim 3 \times 10^{-5} \qquad (30)$$

for leptonic currents in two-body decays.

VI. CONCLUSIONS AND DISCUSSION

The $K_{\mu 3}^0$ decay interaction is found to be vector rather than scalar or tensor in agreement with the $V-A$ theory of weak interactions. This is clear even when energy-dependent form factors are considered.

TABLE I. Summary of results of form-factor analysis.

Assumption	Energy dependence of f_+ and f_-	Best value of parameters	χ^2/DF
Constant form factors	$f_+ =$ constant $f_- =$ constant $\xi = f_-/f_+$	$\xi = 1.2 \pm 0.8$	0.99
Sharp $J=1$ intermediate state of mass M	$f_+ = 1/(M^2 - q^2)$ $f_- = -f_+(M_K^2 - M_\pi^2)/M^2$ $\xi_M = -(M_K^2 - M_\pi^2)/M^2$	$M = 540_{-70}^{+140}$ MeV $\xi_M = -0.8 \pm 0.3$	1.11
Linearly varying form factors	$f_+ = 1 + A_+(q^2/M_\pi^2)$ $f_- = \xi_0 + A_-(q^2/M_\pi^2)$	$A_+ = -0.1$ $A_- = -0.6$ $\xi_0 = 5.6$ (For limits see Fig. 9)	0.92
Sharp $J=0$ intermediate state of mass M_0	$f_+ =$ constant $f_- = f_+(M_K^2 - M_\pi^2)/(M_0^2 - q^2)$	$M_0 = 570_{-70}^{+160}$ MeV	1.03

The two form factors of the vector interaction are found to be consistent with several possible theoretical models for their behavior. If we assume constant form factors, their ratio is found to be $\xi = 1.2 \pm 0.8$. With the assumption of a $J=1$ intermediate K-π state of mass M, we find $M = 540_{-70}^{+140}$ MeV. With a $J=0$ state, we find $M_0 = 570_{-70}^{+160}$ MeV. If the form factors are assumed to be linearly varying, we obtain the results shown in Fig. 9. A summary of the analysis of the form factors is given in Table I.

When the data are compared with the available K_{e3}^0 decay data, the values obtained are consistent with μ-e universality.

It appears that there may be some difference between the K^0 and K^+ leptonic decays. Measurements of K^+ decay[18-25] favor ξ near zero rather than 1.2 or $M(J=1) > 1000$ MeV rather than 540 MeV. An actual difference between the two would imply that $\Delta I = \frac{3}{2}$ currents play an appreciable role in the decays.

ACKNOWLEDGMENTS

We wish to acknowledge the many contributions of Dr. A. Wattenberg to the planning and analysis of this experiment. The assistance and cooperation of the staff at Brookhaven National Laboratory is greatly appreciated. We wish to also thank Dr. William Wenzel of the Lawrence Radiation Laboratory for arranging for the loan of the analyzing magnet.

APPENDIX A: K_2^0 BEAM ENERGY SPECTRUM

In order to calculate the efficiencies described in Sec. IV, the energy spectrum of the decaying K_2^0's must be known. We find this spectrum by observing the energies of the detected K's and correcting the observations with efficiencies calculated at the various energies.

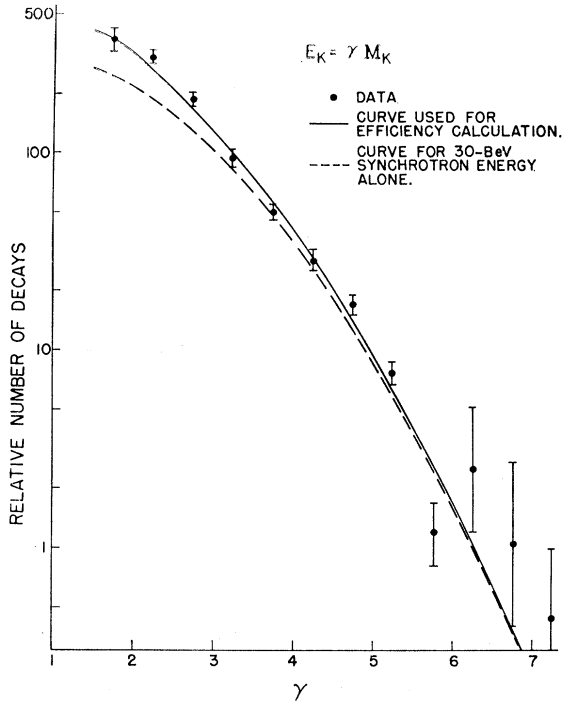

FIG. 10. The observed energy spectrum of the K's decaying in the vacuum pipe 67 ft. from the target in the 30° beam. The solid curve and the data points are for the data taken at 20, 25, and 30 BeV combined.

We assume that the K's at 30° are produced at the beryllium wire target according to the formula

$$\text{Prod}(\beta\gamma) \propto \exp-[A(\beta\gamma)+B(\beta\gamma)^2]\xi, \qquad \text{(A1)}$$

where $(\beta\gamma)\equiv P_K/M_K$, and A and B are parameters to be determined. If the production occurs according to (A1), then the number that decay in the vacuum pipe (67 ft away) will be

$$\text{Decay}(\beta\gamma) \propto \frac{(\text{Prod})}{(\beta\gamma)} e^{-1.03/(\beta\gamma)}. \qquad \text{(A2)}$$

In order to determine A and B, we first pick reasonable values arbitrarily. Then, using the calculated efficiencies at the various K energies and the vector matrix element, we compute the expected distribution of γ_K for the lower E_K solutions to the data. The parameters A and B are then adjusted until good agreement is obtained with the observed low γ distribution.

We find good agreement with the 30-BeV portion of the data with

$$A=-0.34, \quad B=0.172. \qquad \text{(A3)}$$

The corresponding curve for the spectrum of K's decaying at the vacuum pipe [formula (A2)] is shown in Fig. 10 by the dashed curve. The values obtained for the parameters do not depend critically on the form of the vector interaction assumed.

To account for the portion of the data taken at 20 and 25 BeV, we have added three terms of the form (A1):

$$\begin{aligned}\text{Prod}_{30+25+20}(\beta\gamma) &= \text{Prod}_{30}(\beta\gamma)+(0.080)\text{Prod}_{30}[(30/25)\beta\gamma] \\ &\quad +(0.170)\text{Prod}_{30}[(30/20)\beta\gamma]. \qquad \text{(A4)}\end{aligned}$$

The spectrum of decaying K's calculated from (A4) and (A2) is shown by the solid curve in Fig. 10. This is the curve used to obtain the relative weights needed for the efficiency calculation.

If we take $B=0.172$ as fixed, we find the error in A: $A=-0.34\pm0.10$.

As a check on the method of obtaining A and B, and of accounting for the 20- and 25-BeV portions of the data, we have calculated the number of decays occurring at the various values of γ, including corrections for the efficiencies and the kinematical ambiguity. This calculation involves inversion of efficiency matrices similar to those used to obtain the "corrected data" in Sec. IV. The results of the calculation (using the $K_{\mu 3}$ events at all three energies) are plotted as data points on Fig. 10. We see reasonable agreement with the solid line.

The same values of A and B were found to be consistent with the K_{e3} data of Fisher[16] (all at 30 BeV).